

# Design and optimization of an advanced time-of-flight neutron spectrometer for deuterium plasmas of the large helical device

Cite as: Rev. Sci. Instrum. **92**, 053547 (2021); <https://doi.org/10.1063/5.0043766>  
 Submitted: 11 January 2021 • Accepted: 08 May 2021 • Published Online: 24 May 2021

 Yimo Zhang,  Lijian Ge, Zhimeng Hu, et al.

## COLLECTIONS

Paper published as part of the special topic on [Proceedings of the 23rd Topical Conference on High-Temperature Plasma Diagnostics](#)



View Online



Export Citation



CrossMark

## ARTICLES YOU MAY BE INTERESTED IN

[Neutron-induced signal on the single crystal chemical vapor deposition diamond-based neutral particle analyzer](#)

Review of Scientific Instruments **91**, 113304 (2020); <https://doi.org/10.1063/5.0020460>

[Fast deuteron diagnostics using visible light spectra of  \$^3\text{He}\$  produced by deuteron-deuteron reaction in deuterium plasmas](#)

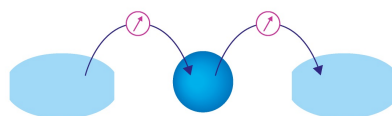
Review of Scientific Instruments **92**, 053524 (2021); <https://doi.org/10.1063/5.0034683>

[Observations of visible argon line emissions and its spatial profile from Aditya-U tokamak plasma](#)

Review of Scientific Instruments **92**, 053548 (2021); <https://doi.org/10.1063/5.0043877>

Webinar

Interfaces: how they make or break a nanodevice



March 29th – Register now



Zurich  
Instruments



# Design and optimization of an advanced time-of-flight neutron spectrometer for deuterium plasmas of the large helical device

Cite as: Rev. Sci. Instrum. 92, 053547 (2021); doi: 10.1063/5.0043766

Submitted: 11 January 2021 • Accepted: 8 May 2021 •

Published Online: 24 May 2021



View Online



Export Citation



CrossMark

Yimo Zhang,<sup>1</sup> Lijian Ge,<sup>1</sup> Zhimeng Hu,<sup>1,2</sup> Jiaqi Sun,<sup>1</sup> Xiangqing Li,<sup>1</sup> Kunihiro Ogawa,<sup>3</sup> Mitsutaka Isobe,<sup>3</sup> Siriyaporn Sangaroon,<sup>3</sup> Longyong Liao,<sup>1</sup> Danke Yang,<sup>1</sup> Giuseppe Gorini,<sup>2,4</sup> Massimo Nocente,<sup>2,4</sup> Marco Tardocchi,<sup>4</sup> and Tieshuan Fan<sup>1,a)</sup>

## AFFILIATIONS

<sup>1</sup> State Key Laboratory of Nuclear Physics and Technology, Peking University, Beijing 100871, China

<sup>2</sup> Dipartimento di Fisica “G. Occhialini,” Università degli Studi di Milano-Bicocca, Milano 20126, Italy

<sup>3</sup> National Institute for Fusion Science, 322-6 Oroshi-cho, Toki 509-5292, Japan

<sup>4</sup> Institute for Plasma Science and Technology, National Research Council, Milan 20125, Italy

**Note:** Paper published as part of the Special Topic on Proceedings of the 23rd Topical Conference on High-Temperature Plasma Diagnostics.

**a)** Author to whom correspondence should be addressed: [tsfan@pku.edu.cn](mailto:tsfan@pku.edu.cn)

## ABSTRACT

A time-of-flight neutron spectrometer based on the Time-Of-Flight Enhanced Diagnostic (TOFED) concept has been designed and is under development for the Large Helical Device (LHD). It will be the first advanced neutron spectrometer to measure the 2.45 MeV D–D neutrons (DDNs) from helical/stellarator plasmas. The main mission of the new TOFED is to study the supra-thermal deuterons generated from the auxiliary heating systems in helical plasmas by measuring the time-of-flight spectra of DDN. It will also measure the triton burnup neutrons (TBNs) from the d+t reactions, unlike the original TOFED in the EAST tokamak. Its capability of diagnosing the TBN ratios is evaluated in this work. This new TOFED is expected to be installed in the basement under the LHD hall and shares the collimator with one channel of the vertical neutron camera to define its line of sight. The distance from its primary scintillators to the equatorial plane of LHD plasmas is about 15.5 m. Based on Monte Carlo simulation by a GEANT4 model, the resolution of the DDN energy spectra is 6.6%. When projected onto the neutron rates that are typically obtained in LHD deuterium plasmas (an order of  $10^{15}$  n/s with neutral beam injection), we expect to obtain the DDN and TBN counting rates of about  $2.5 \cdot 10^5$  counts/s and 250 counts/s, respectively. This will allow us to analyze the DDN time-of-flight spectra on time scales of 0.1 s and diagnose the TBN emission rates in several seconds with one instrument, for the first time in helical/stellarator plasmas.

Published under license by AIP Publishing. <https://doi.org/10.1063/5.0043766>

## I. INTRODUCTION

Neutrons produced from D–D and D–T reactions carry information about the kinematic state of fusion fuels in plasmas. Among magnetic confined fusion devices such as tokamaks, neutron diagnostics have been widely adopted.<sup>1</sup> In particular, advanced Neutron Emission Spectroscopy (NES) diagnostics, such as the MPR<sup>2</sup> and the time-of-flight neutron spectrometer TOFOR<sup>3</sup> at the Joint European Torus, have proven to be powerful instruments to understand the behavior of energetic particles<sup>4–8</sup> in fusion experiments, which is of relevance for burning plasma devices, such as ITER.<sup>9,10</sup>

With regard to the present stellarators and helical devices, the Large Helical Device (LHD) started its first deuterium experimental campaign in 2017, in order to explore the related fusion plasma physics and engineering challenges.<sup>11</sup> There are already rather comprehensive neutron diagnostics at the LHD, including neutron flux monitors, neutron activation systems, a vertical neutron camera, and scintillating-fiber detectors, which all operate with good performance during the recent experiments.<sup>12</sup> The recorded neutron emission rates at the LHD reach more than  $10^{15}$  n/s<sup>13</sup> due to a large number of fast ions, mainly generated from the external power by the auxiliary heating system.

In order to advance our knowledge on the fast ion behaviors in the helical fusion plasmas, a new advanced time-of-flight neutron spectrometer based on the TOFED (Time-Of-Flight Enhanced Diagnostic) concept<sup>14</sup> will be developed at the LHD, and it will be the first advanced neutron spectrometer for a helical/stellarator device. The TOFED neutron spectrometer, which originates from the TOFOR concept but has an improved efficiency and energy resolution due to its double-ring secondary scintillator array, has been developed and put into successful operations at the EAST tokamak for the studies of fast ions from the NBI (Neutral Beam Injection) and ICRF (Ion Cyclotron Resonance Frequency) heating systems.<sup>15–18</sup> Moreover, time-resolved triton burnup diagnosis has been conducted by the measurements of the 14 MeV D–T neutrons, such as using the scintillating-fiber detectors. According to the recent experimental results at LHD, the yields of the Triton Burnup Neutrons (TBNs) exceed  $10^{12}$  n/s, up to 0.5% of the D–D neutrons (DDNs).<sup>19</sup> It will be an attractive application of the TOFED-type neutron spectrometer at the LHD if this new instrument can appropriately respond to both DDN and TBN from the helical fusion plasmas.

In this paper, the new TOFED neutron spectrometer at the LHD is described. Section II briefly introduces the basic principle of the neutron time-of-flight measurement. In Sec. III, the TOFED-type spectrometer concept at the LHD is discussed in detail. These results are summarized in Sec. IV.

## II. TIME-OF-FLIGHT PRINCIPLE

The time-of-flight (TOF) neutron spectrometer consists of two sets of plastic scintillators in which neutrons can collide with protons by the elastic scattering process, shown in Fig. 1. Assuming that all the scintillators are tangential to a sphere (with a radius  $R$ ), the collimated neutrons are scattered in the primary scintillators (S1).

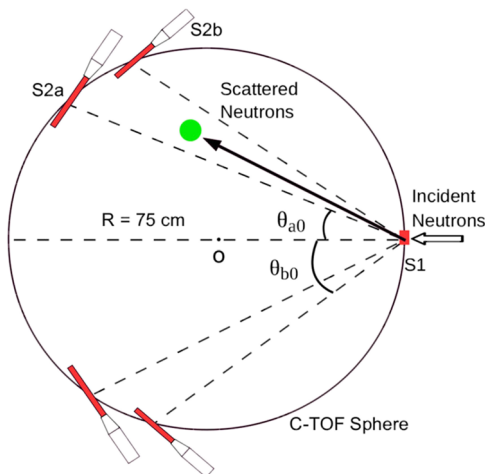


**FIG. 1.** Schematic of the principle of the TOFED concept. The two sets of plastic scintillators S1 (primary) and S2 (secondary) are arranged on the surface of the C-TOF sphere. When the collimated neutron flux perpendicularly hits the S1 scintillator, some neutrons will be deflected to the S2 detectors and their interaction is recorded. Under these circumstances, the time-of-flight of the scattered neutrons is only determined by the incident neutrons' energy regardless of the different flight path scattered neutrons may follow from S1 to S2.

If one neutron with energy  $E_n$  hits a proton in S1 in a single scattering with a deflection within the solid angle defined by the size of S2s of the double ring, i.e.,  $n + p \rightarrow p_r + n'$ , and then the scattered neutron reaches the S2 scintillators, it results in

$$t_{tof} = \frac{2R \cos \theta}{v'_n}, \quad (1)$$

$$E'_n = E_n \cos^2 \theta = \frac{m_n v'_n{}^2}{2}, \quad (2)$$

where  $\theta$  is the scattering angle,  $v'_n$  is the velocity of the neutron after the first scattering,  $m_n$  is the mass of the neutron, and  $t_{tof}$  denotes the time-of-flight of the scattered neutron. Therefore, energies of the incident neutron and the recoil proton inside S2,  $E_n$  and  $E_p$ , are obtained as

$$E_n = \frac{2m_n R^2}{t_{tof}^2}, \quad (3)$$

$$E_p = E_n \sin^2 \theta = \frac{2m_n R^2}{t_{tof}^2} \sin^2 \theta. \quad (4)$$

This implies that the scattered neutrons born from the incoming neutrons with the same energy  $E_n$  take the same time to reach S2 irrespective of their scattering angle  $\theta$ . This is the so-called constant time-of-flight (C-TOF) sphere principle. Neutrons scattering multiple times or scattering on carbons inside S1 will, however, break this principle.<sup>20</sup> In the TOFED case, the radius of the C-TOF is 1.5 m. There are five parallel layers of S1 scintillators and 80 S2 scintillators, which are split into two rings, shown in Fig. 2. 40 S2 scintillators constitute the upper ring (S2a) and cover the neutron scattering angles from  $20^\circ$  to  $31^\circ$ , while these angles are  $31^\circ < \theta < 40^\circ$  for the other 40 scintillators of the bottom ring (S2b). The neutron scattering angles determine a range for the scattered proton energy  $E_p$  that can be released in S1, given  $E_n$ . The effective neutron events can thus be discriminated from the multiple scattering events or carbon scattering events by the time-of-flight and recoiled proton energy, which constitute the principle of the double kinematic selection (DKS) method.<sup>15,21</sup>

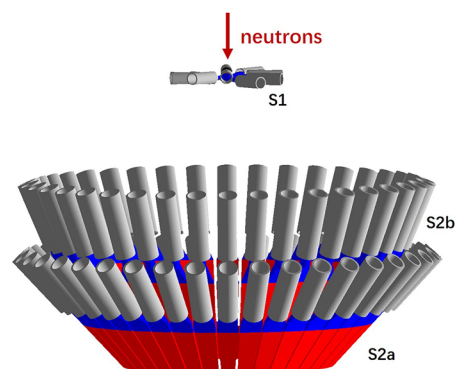


**FIG. 2.** The model for LHD-TOFED includes five layers of S1 scintillators, 40 upper-ring (S2a) and 40 bottom-ring (S2b) scintillators, and their light guides and photomultiplier tubes.

### III. TOFED-TYPE SPECTROMETER AT THE LHD

The LHD is one of the largest superconducting helical devices with a major radius/minor radius of 3.9 m/~0.6 m. Its NBI heating system consists of three tangentially injected and two radially injected neutral beams with maximum beam energies of around 180 and 60 keV, and the total NBI power can be of up to 30 MW. The ICRF system with a total power of about 6 MW is also a main heating source at the LHD.<sup>11</sup> Analyzing the neutron spectra to obtain the velocity distribution of the fuel ions, the TOFED-type neutron spectrometer (mentioned as LHD-TOFED) is primarily aimed at studying fast ions produced by auxiliary heating in the LHD plasmas.

#### A. Line of sight

LHD-TOFED is expected to be installed in the basement under the LHD hall and shares one of the collimators with a view line that passes through a concrete shielding. This collimator is the middle channel of the Vertical Neutron Camera (VNC),<sup>22</sup> which is installed above the LHD-TOFED. The collimator locates at the LHD lower port (the so-called 2.5L port) at a major radius of 3.72 m. The distance from the equatorial plane of the LHD plasma to the S1 scintillator of LHD-TOFED is at least 15.5 m, as sketched in Fig. 3. This collimator with a radius of 30 mm defines a line of sight with a divergence of no more than  $0.23^\circ$  and gives the

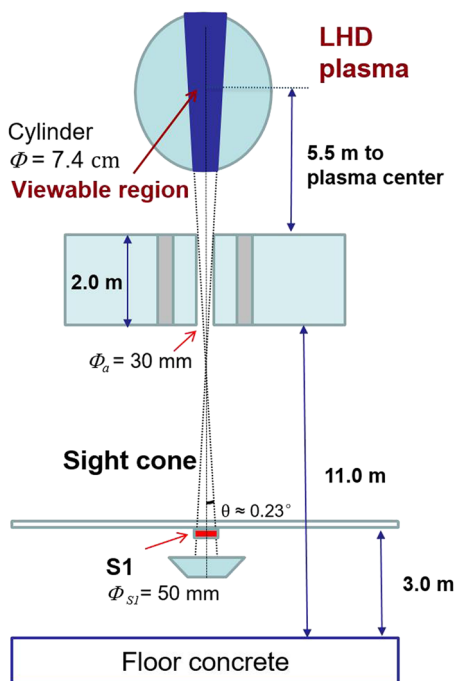


**FIG. 3.** The LHD-TOFED is expected to be installed under the LHD plasmas. A hole with a radius of 30 mm through the 2-m-thick basement is used as the collimator and radiation shielding. The distance from the equatorial plane of LHD plasmas to the S1 scintillator of LHD-TOFED is at least 15.5 m. This collimator, which is originally used by the vertical neutron camera, defines a line of sight with a divergence of no more than  $0.23^\circ$  and gives LHD-TOFED a viewable region, which can be approximately regarded as a cylinder with a radius of about 7.4 cm.

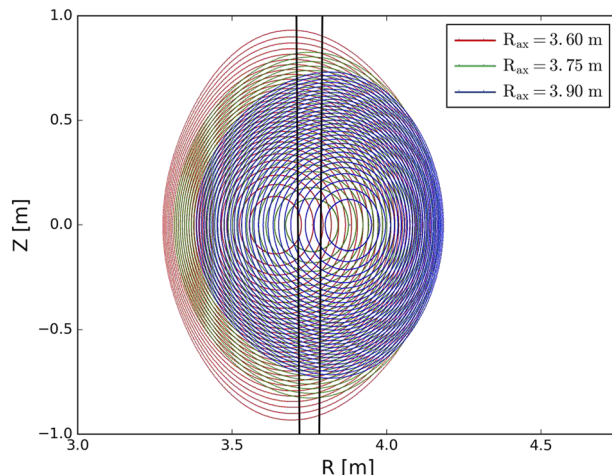


**FIG. 4.** The line of sight of the LHD-TOFED gives an approximately cylindrical viewing region (between the black lines). For the three typical magnetic configurations ( $R_{ax} = 3.6$  m in red,  $R_{ax} = 3.75$  m in green, and  $R_{ax} = 3.9$  m in blue), the LHD-TOFED can always collect the fusion neutrons from the helical plasma core.

LHD-TOFED a viewing region, which is approximately a cylinder with a radius of about 7.4 cm. The plasma profile observed by the LHD-TOFED is approximately an ellipse along the vertical major axis.

In LHD, the magnetic configuration can be shifted outward or inward, as illustrated in Fig. 4. During the typical operation regime at the LHD, the radii of the magnetic axis usually range from 3.6 to 3.9 m. In these conditions, the line of sight of the new instrument (black line) can always ensure the observation of a collimated line-integrated neutron flux from the core of the helical plasma where neutrons of almost the largest flux are generated during the NBI-heated discharges.<sup>22</sup>

#### B. Data acquisition

The digital DAQ (data acquisition) system envisaged for the LHD-TOFED is based on compact digitizers that can measure the pulse height and time information of neutron scattering events in S1 and S2. In recent experiments, several NES diagnostics in tokamaks around the world have upgraded the electronics through the employment of digitizers.<sup>23–25</sup> APV8104-14 from Techno AP<sup>26</sup> has been chosen as the reference for the LHD-TOFED. Its main features and parameters are listed in Table I. The communication between this type of digitizer and the computer is established by the TCP/IP protocol. The digital DAQ system can work at counting rates of up to  $10^6$  counts/s at the LHD due to the 2 GB RAM and the

**TABLE I.** The main technical parameters of the APV8104-14 digitizer.

Sampling rate	Number of channels	Bit number	$V_{pp}$	Bandwidth	RAM
1 G samples/s	4	14	$\pm 3$ V	500 MHz	2 GB

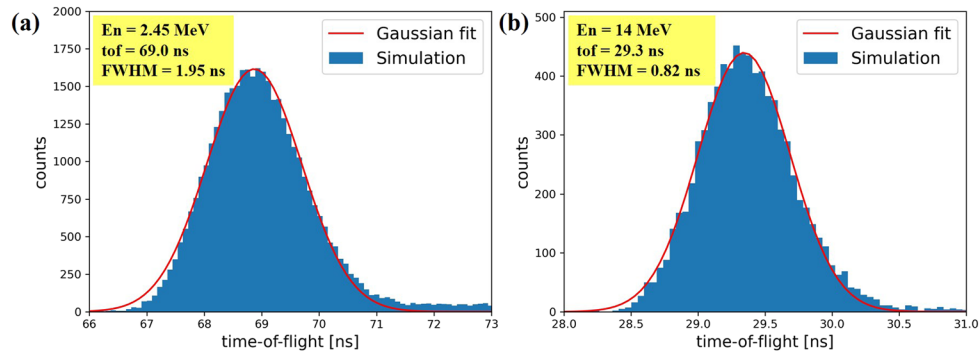


FIG. 5. The simulated time-of-flight spectra for mono-energetic (a) 2.45 and (b) 14 MeV neutrons are shown. The Gaussian fitting curves are plotted in red.

data transmission by optical fibers. A sampling rate of 1G samples/s satisfies the requirements of sub-nanosecond level precision for neutron time-of-flight measurements, combined with the CFD (Constant Fraction Discrimination) method in the off-line data processing.<sup>18,23</sup> The data acquisition set in the mix mode can collect both the pulse shape and triggering time, making it possible to apply the DKS method to improve the signal-to-background of the neutron events recorded in the time-of-flight spectra. More detailed work including the integrated design, the time synchronization, and the setting of the parameters of the whole digital DAQ system will be conducted in the future.

### C. Response to DDN and TBN

Since the LHD has reached high neutron rates in view of its auxiliary heating system, D–D fusion neutrons of a comparable rate to those of large tokamaks such as JET and considerable triton burn-up neutrons are emitted from their helical plasmas. A Monte Carlo model of neutron transport from the plasma to the LHD-TOFED

has been developed using the GEANT4 code.<sup>27</sup> In the simulation, the materials of scintillators are EJ228 for S1 and EJ200 for S2, which are the same with those of the original TOFED.<sup>23</sup> The performances of two types of scintillators have been previously investigated, and their light output function is known from calibration experiments at neutron accelerators.<sup>15,16</sup> Their response to both 2.45 MeV DDN emission and 14 MeV TBN emission has also been evaluated as described in the following.

The overall geometry of the scintillator array of LHD-TOFED is responsible for a Gaussian shape broadening of the time-of-flight spectrum resulting from a collimated beam of 2.45 MeV mono-energetic neutrons as input. By fitting the simulation results, we obtain that the DDN peak on the  $t_{tof}$  axis is located at around 69.0 ns, while the TBN peak is at 29.3 ns, as shown in Fig. 5. The FWHMs for DDN and TBN spectra are 1.95 and 0.82 ns, respectively. By taking into account the contribution from the digital DAQ system and light transmission from the scintillators to the photo-multiplier tube based on the experience of the TOFOR at

TABLE II. The energy resolutions of LHD-TOFED for DDN and TBN.

$E_n$ (MeV)	$t_{tof}$ (ns)	FWHM from geometry (ns)	FWHM from light propagation (ns)	FWHM from DAQ (ns)	FWHM in total (ns)	Energy resolution (%)
2.45	69.0	1.95	0.6	1.0	2.27	6.6
14.0	29.3	0.82	0.6	1.0	1.42	9.7

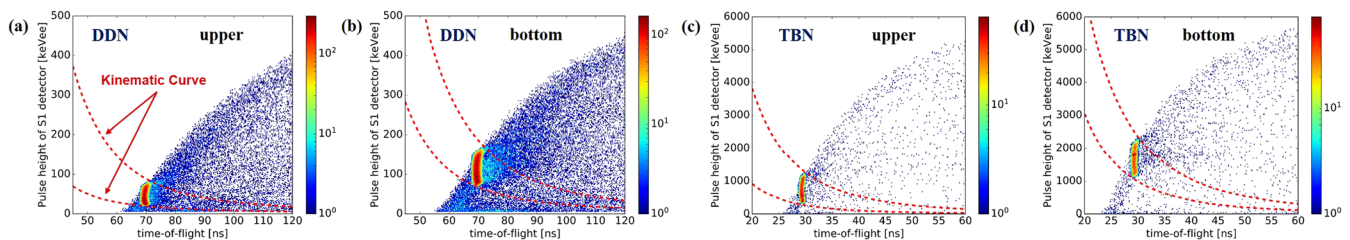


FIG. 6. The 2D plots of time-of-flight vs pulse height [the pulse heights are expressed by light output in the scintillators, in units of keVee (keV electron equivalent), which means the charges induced by a 1 keV electron in the scintillator] in S1 scintillators of mono-energetic neutrons are exemplified. (a) 2.45 MeV DDN that can be collected by using the upper-ring S2a scintillators. (b) 2.45 MeV DDN that can be collected by using the bottom-ring S2b scintillators. (c) 14 MeV TBN that can be collected by using the upper-ring S2a scintillators. (d) 14 MeV TBN that can be collected by using the bottom-ring S2b scintillators. The effective single-scattering neutron events concentrate between the kinematic curves (red dotted line), while the background events mainly come from the multiple scattering on nuclei in the scintillators.



**TABLE III.** The estimated neutron counting rates for DDN and TBN at the primary scintillators of the LHD-TOFED.

Neutron type	Neutron flux (n/s.cm <sup>2</sup> )	Area efficiency (cm <sup>2</sup> )	Counting rate (counts/s)
DDN	10 <sup>6</sup>	0.25	2.5 × 10 <sup>5</sup>
TBN	5 × 10 <sup>3</sup>	0.05	250

JET and the TOFED at EAST,<sup>23,28</sup> the total neutron energy resolutions of the LHD-TOFED are estimated to be about 6.6% for DDN and 9.7% for TBN. More details on the contribution of each term to the overall energy resolution of the instrument are given in Table II.

As far as the energy released by single scattered protons in S1 is concerned, this is determined by using Eq. (4) and depends on the range of the neutron scattering angle. In the 2D plot of time-of-flight vs pulse height of the protons in the S1, shown in Fig. 6, we find that the single-scattering neutron events concentrate between two kinematic curves. These depend only on the finite scattering angle range determined by the solid angle covered by S2. Therefore, most events that come from the multiple scattering on nuclei in the scintillators can be filtered by the DKS method. We note that the discrimination capability based on the DKS method is higher for 14 MeV TBN than for 2.45 MeV DDN events, which implies an even better signal-to-background ratio of TBN measurements. By considering the finite geometry of S2, we expect that energies in the range from 20 to 180 keV for the DDN and 300 to 2300 keV for the TBN may be deposited in the S2 scintillators. Hence, there is need for a DAQ system with a dynamic range of three orders of magnitude and with a good signal-to-background ratio to simultaneously measure the DDN and TBN emission with the LHD-TOFED.

In recent experimental campaigns at LHD, the neutron yield reached more than  $1 \times 10^{15}$  n/s and the TBN ratio was up to 0.5%. With the expected vertical line of sight, the neutron fluxes on S1 scintillators of the LHD-TOFED are estimated to be 10<sup>6</sup> n/(s cm<sup>2</sup>) for DDN and  $5 \times 10^3$  n/(s cm<sup>2</sup>) for TBN. Considering the surface of the S1 scintillators facing the incident neutrons, the area efficiencies are obtained from the GEANT4 simulations and presented in Table III. The recorded counting rates of DDN and TBN would be  $2.5 \times 10^5$  counts/s and 250 counts/s, respectively, in which the count rates are possibly sufficient for the diagnosis of the TBN ratio. This will allow studies of the DDN and TBN emission on time scales of 1/10 and several seconds for the two components, respectively.

#### IV. CONCLUSION

A TOFED-type neutron spectrometer (LHD-TOFED) is under development for the LHD. Four S1 and four S2 scintillators were installed and operated during the deuterium plasma experiment campaign in 2019. The preliminary results demonstrate that a dedicated shielding is prerequisite for the employment of LHD-TOFED due to a high scattering neutron and gamma flux in the LHD basement. The shielding has been designed recently, with which the ambient radiations can be reduced by two orders of magnitude.<sup>29</sup>

The LHD-TOFED will be the first NES diagnostic in a helical/stellarator device. The main mission of the LHD-TOFED is to measure the 2.45 MeV D–D neutrons for diagnosing energetic ion behaviors in helical/stellarator plasmas, with the additional capability to measure 14 MeV neutrons born in triton burnup d+t reactions. By using a digital data acquisition system and the double kinematic selection method, a sufficient signal-to-background ratio for simultaneously measuring the DDN and TBN components can be obtained. The LHD-TOFED will be one of the main diagnostics for studies of fast ions in deuterium helical plasmas at LHD and will also serve as a complementary diagnostic for investigations on the confinement of MeV range tritons born in DD fusion reactions.

#### ACKNOWLEDGMENTS

This work was supported by the National MCF Energy R & D Program (Grant Nos. 2019YFE03040000, 2013GB106004, and 2012GB101003), the National Key Research and Development Program of China (Grant Nos. 2016YY0200805 and 2017YFF0206205), the State Key Program of National Natural Science of China (Grant No. 11790324), and the User with Excellence Program of Hefei Science Center CAS (Grant No. 2020HSC-UE012).

#### DATA AVAILABILITY

The data that support the findings of this study are available from the corresponding author upon reasonable request.

#### REFERENCES

- 1 B. Wolle, *Phys. Rep.* **312**, 1 (1999).
- 2 G. Ericsson, L. Ballabio *et al.*, *Rev. Sci. Instrum.* **72**, 759 (2001).
- 3 M. Gatun Johnson *et al.*, *Nucl. Instrum. Methods Phys. Res., Sect. A* **591**, 417 (2008).
- 4 J. Källne *et al.*, *Phys. Rev. Lett.* **85**, 1246 (2000).
- 5 C. Hellesen *et al.*, *Plasma Phys. Controlled Fusion* **52**, 085013 (2010).
- 6 C. Hellesen, *et al.*, *Nucl. Fusion* **53**, 113009 (2013).
- 7 J. Eriksson *et al.*, *Nucl. Fusion* **55**, 123026 (2015).
- 8 C. Hellesen *et al.*, *Nucl. Fusion* **58**, 056021 (2018).
- 9 N. N. Gorelenkov, S. D. Pinches, and K. Toi, *Nucl. Fusion* **54**, 125001 (2014).
- 10 M. Nocente, *J. Fusion Energy* **38**, 291 (2019).
- 11 M. Osakabe *et al.*, *Fusion Sci. Technol.* **72**, 199–210 (2017).
- 12 M. Isobe *et al.*, *IEEE Trans. Plasma Sci.* **46**, 2050 (2018).
- 13 K. Ogawa, *et al.*, *Plasma Phys. Controlled Fusion* **60**, 095010 (2018).
- 14 X. Zhang *et al.*, *Nucl. Fusion* **54**, 104008 (2014).
- 15 X. Y. Peng *et al.*, *Rev. Sci. Instrum.* **85**, 11E112 (2014).
- 16 X. Y. Peng *et al.*, *Rev. Sci. Instrum.* **87**, 11D836 (2016).
- 17 L. J. Ge *et al.*, *Rev. Sci. Instrum.* **89**, 10I143 (2018).
- 18 Y. Zhang, Ph.D. thesis, Peking University, 2020 (in Chinese).
- 19 K. Ogawa *et al.*, *Nucl. Fusion* **58**, 034002 (2018).
- 20 G. Gorini and J. Källne, *Rev. Sci. Instrum.* **63**, 4548 (1992).
- 21 X. Zhang *et al.*, *Rev. Sci. Instrum.* **85**, 043503 (2014).
- 22 K. Ogawa *et al.*, *Rev. Sci. Instrum.* **89**, 113509 (2018).
- 23 Z. J. Chen, X. Y. Peng *et al.*, *Rev. Sci. Instrum.* **85**, 11D830 (2014).
- 24 M. Skiba *et al.*, *Nucl. Instrum. Methods Phys. Res., Sect. A* **833**, 94 (2016).
- 25 L. J. Ge, Z. M. Hu *et al.*, *Plasma Phys. Controlled Fusion* **60**, 095004 (2018).
- 26 See [http://www.techno-ap.com/index\\_e.html](http://www.techno-ap.com/index_e.html) for Techno AP.
- 27 S. Agostinelli, *Nucl. Instrum. Methods Phys. Res., Sect. A* **506**, 250–303 (2003).
- 28 L. Giacomelli, Ph.D. thesis, Acta Universitatis Upsaliensis, Uppsala, (2007).
- 29 S. Sangaroon *et al.*, *Fusion Eng. Des.* **166**, 112296 (2021).